




Killing of *Anopheles stephensi* mosquitoes by selective triketone inhibitors of 4-hydroxyphenylpyruvate dioxygenase depends on a high protein meal

Matěj Kučera^{a,b}, David Hartmann^a, James J. Valdés^{a,c}, Adéla Palusová^a, Avinash Sheshachalam^d, Marnix Vlot^d, Martijn W. Vos^d, Koen J. Dechering^{d,*}, Jan Perner^{a,**} 

^a Institute of Parasitology, Biology Centre, Czech Academy of Sciences, České Budějovice, Czech Republic

^b Faculty of Science, University of South Bohemia, České Budějovice, Czech Republic

^c Centre Algatech, Institute of Microbiology, Czech Academy of Sciences, Novohradská 237, 37901 Třeboň, Czech Republic

^d TropiQ Health Sciences, Transistorweg 5, 6534 AT Nijmegen, the Netherlands

ARTICLE INFO

Keywords:

Anopheles stephensi

Malaria vector control

4-Hydroxyphenylpyruvate dioxygenase (HPPD)

Nitisinone

Tyrosine catabolism

Blood-feeding mosquitoes

ABSTRACT

The malaria vector *Anopheles stephensi* has expanded from Asia into Eastern Africa, posing a growing global health threat due to its adaptive biology and increasing resistance to conventional control methods. Here, we characterise 4-hydroxyphenylpyruvate dioxygenase (HPPD), a crucial enzyme in the tyrosine degradation pathway, and demonstrate its potential as a novel drug target in *An. stephensi*. Homology modeling combined with molecular dynamics simulations confirmed that key inhibitor-binding residues are highly conserved across mosquito HPPDs and predicted potent inhibition by triketone-based compounds. Using cell-based assay with codon-optimized recombinant expression in *Escherichia coli*, we screened several triketone and diketone nitrile HPPD inhibitors and identified nitisinone as the most potent inhibitor, displaying nanomolar-range IC₅₀ values. Membrane feeding assays showed that nitisinone's insecticidal activity relies on ingestion of a high-protein meal, with haemoglobin identified as the potent dietary factor driving toxicity. These results highlight HPPD inhibition as a promising blood-meal-dependent vector control strategy specifically targeting haematophagous mosquitoes.

1. Introduction

Mosquito-borne diseases continue to represent a significant global public health challenge, with malaria being the most prominent in terms of morbidity, mortality, and socioeconomic burden. In 2022 alone, malaria caused an estimated 249 million cases and 608,000 deaths globally (Venkatesan, 2024). The causative parasite, *Plasmodium* spp. are primarily transmitted in sub-Saharan Africa by *Anopheles gambiae* (Toure et al., 2004). *Anopheles stephensi* is an emerging threat and a main malaria vector in South Asia and the Middle East (Taylor et al., 2024). Alarming, this mosquito has spread to Eastern Africa and is rapidly expanding westward (Emiru et al., 2023). Vector control, largely via insecticides, has been the cornerstone of malaria prevention. As malaria control has continued to rely on a few classes of insecticides, mosquitoes have evolved multiple resistance mechanisms, jeopardizing the effectiveness of existing tools (Hancock et al., 2024; Churcher et al., 2016). Current mosquito control interventions predominantly have relied on

insecticides targeting ion channels of insect nervous system (ffrench-Constant et al., 2016), underscoring a need for novel molecular targets with alternative modes of action to sustain and advance vector control efforts. The momentum for identifying novel targets in disease-vectors is now accelerated by new physiological insights, now achievable through comprehensive genomic and transcriptomic datasets (Cerqueira de Araujo et al., 2025; Neafsey et al., 2015; Ribeiro et al., 2014). Advances in sequencing technologies have illuminated previously inaccessible aspects of mosquito biology, highlighting vulnerabilities such as metabolic pathways and blood meal-activated processes that can be exploited with precision. Leveraging these detailed molecular insights not only broadens the spectrum of potential insecticidal targets but also promises greater specificity in mosquito control strategies.

Insects that feed on vertebrate blood possess unique metabolic and physiological adaptations to exploit this protein-rich meal. Blood ingestion triggers digestion, nutrient assimilation, egg maturation, and

This article is part of a special issue entitled: Molecular biology of insecticide models published in Insect Biochemistry and Molecular Biology.

* Corresponding author.

** Corresponding author.

E-mail addresses: k.dechering@tropiq.nl (K.J. Dechering), perner@paru.cas.cz (J. Perner).

<https://doi.org/10.1016/j.ibmb.2025.104361>

Received 12 May 2025; Received in revised form 2 July 2025; Accepted 13 July 2025

Available online 18 July 2025

0965-1748/© 2025 Elsevier Ltd. All rights are reserved, including those for text and data mining, AI training, and similar technologies.

detoxification. These blood-specific pathways are essential for mosquito survival and reproduction yet are absent in non-haematophagous insects, offering an untapped reservoir of selective insecticide targets (Sterkel et al., 2017). Targeting such blood-meal-dependent vulnerabilities could achieve high specificity for vector species while reducing non-target effects, addressing both efficacy and environmental safety in vector control. One such pathway of interest is tyrosine catabolism, a process essential for safely metabolising the excess amino acids derived from haemoglobin digestion (Sterkel et al., 2016). Central to this pathway is 4-hydroxyphenylpyruvate dioxygenase (HPPD), an iron-dependent enzyme that converts 4-hydroxyphenylpyruvate into homogentisic acid. HPPD has been extensively studied in the context of plant herbicides and human metabolic disorders, but the molecular details of the mode of action are not fully resolved.

Here, we complement previous observations with molecular insights of HPPD inhibition, supporting blood meal-activated strategy for malaria vector control. We show that HPPD is highly conserved across mosquito species and validate it as a molecular target in *An. stephensi* mosquitoes. Through homology modeling and molecular dynamics, we confirmed that mosquito HPPD shares some key inhibitor-binding features with its human and plant counterparts, explaining the susceptibility of mosquito HPPD to triketone inhibitors. Using heterologous expression, we screened triketone and diketone nitrile HPPD inhibitors and identified the triketone nitisinone as the most potent inhibitor of mosquito HPPD, with nanomolar activity. Our membrane feeding assays revealed that nitisinone's insecticidal effect on *An. stephensi* is strictly contingent upon blood feeding, emphasising high protein meal as a critical requirement driving the toxicity. Our work highlights selectivity of inhibition of mosquitoes HPPD by triketone inhibitors and specificity for blood-meal activation of the inhibition potential, offering viable strategy for controlling malaria vectors.

2. Results

2.1. 4-Hydroxyphenylpyruvate dioxygenase is highly conserved across mosquito species

We identified a single-copy HPPD gene in the genomes of multiple mosquito species (*Anopheles*, *Aedes*, *Culex* spp.), consistent with the enzyme's broad conservation from bacteria and plants to animals. Despite considerable primary sequence divergence (only ~34 % amino acid identity between *Arabidopsis thaliana* HPPD and *An. stephensi* HPPD; see Fig. 1A), the amino acid residues known to be important for inhibitor binding are highly conserved in mosquito HPPDs. Sequence alignment revealed that the catalytic His-His-Glu triad (corresponding to His183, His266, Glu349 in human HPPD (Lin et al., 2019b)) is strictly conserved (Fig. 1A). Conservation of the triad indicates herbicidal and human HPPD inhibitors may be broadly effective, acting on HPPD enzymes from diverse species. Other key residues that determine inhibitor affinity in mammalian and plant HPPDs are also present in mosquitoes. For example, Tyr221 and Leu224 (human HPPD numbering) are conserved in mosquitoes; mutation of these residues to alanine in human HPPD causes a significant loss of 2-(2-nitro-4-trifluoromethylbenzoyl)-1, 3-cyclohexanedione (nitisinone or NTBC) binding affinity (Liu et al., 2020). Likewise, positions that interact hydrophobically with the cyclohexane ring of triketone inhibitors (Val185, Val228, Pro239, Phe359 in human) or bind the aromatic trifluoromethyl group of nitisinone and related herbicides (Leu323, Phe336, Phe364, Leu367) are largely invariant in mosquito HPPD (Lin et al., 2019b). Two phenylalanine residues (Phe336 and Phe364 in human) form a π -stacking around the aromatic ring of nitisinone in the enzyme-inhibitor complex, a feature proposed to contribute to nitisinone's high affinity for HPPD (Neidig et al., 2005). The orientation of Phe368 potentially regulates inhibitor's access to the active site by modulating binding kinetics (Lin et al., 2019b). Our sequence and structural analysis thus indicate that HPPD enzymes in mosquitoes possess a conserved active site architecture, making them amenable to inhibition by the same compounds that

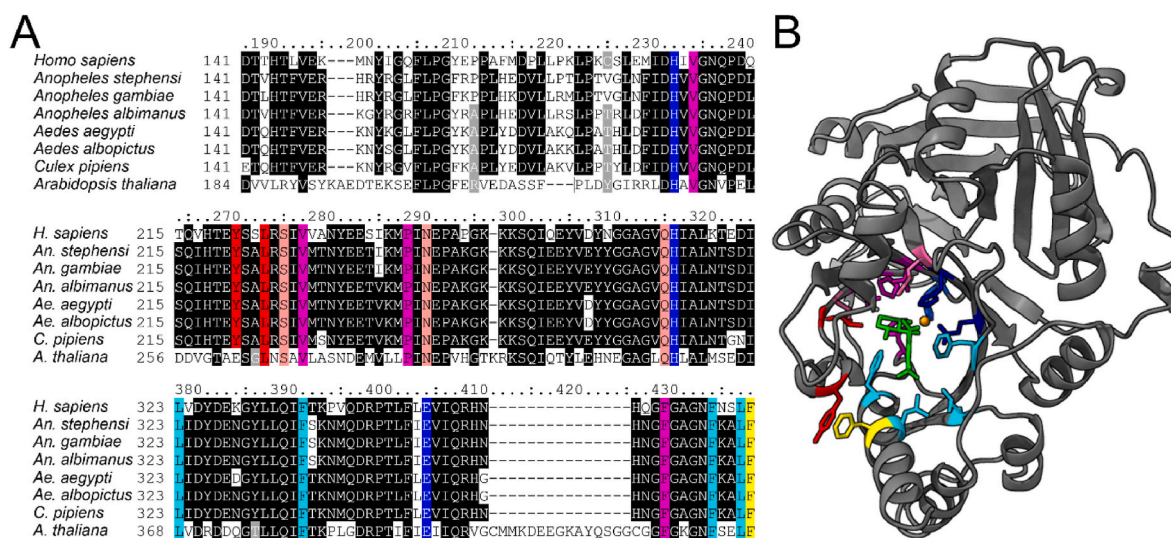


Fig. 1. Sequence alignment and 3D structure of HPPD from *Anopheles stephensi*. (A) Key regions of HPPD amino acid sequence alignment of HPPD from multiple species, including six mosquito species, human, and *Arabidopsis thaliana*, a plant commonly used in herbicide studies. blue: His183, His266, Glu349 triad, red: Tyr221 and Leu224, magenta: Val185, Val228, Pro239, Phe359, cyan: Leu323, Leu367, Phe336, Phe364, yellow: Phe368, pink: Ser 226, Asn 241, Gln 265. The numbering corresponds to human and mosquito HPPD sequences. Accession numbers for the HPPD sequences used in this alignment are as follows: *Homo sapiens* (AAC73008.1), *Anopheles stephensi* (XP_035912472.1), *An. gambiae* (XP_318007.3), *An. albimanus* (XP_035789652.1), *Aedes aegypti* (XP_001649088.2), *Ae. albopictus* (XP_019555351.2), *Culex pipiens* (XP_039429287.1), and *A. thaliana* (NP_172144.3). For the complete protein alignment, please refer to the [Supplementary Fig. S1](#). (B) The 3D structure of HPPD from *An. stephensi*, modeled using the SwissModel server with human HPPD complexed with nitisinone as a template (PDB entry 8IM2). The complexed nitisinone (green) and an Fe ion (orange sphere) are located within the enzyme's active site. Residues critical for inhibitor binding are colored according to the alignment in panel B. The model was visualised and colored using UCSF ChimeraX. (For interpretation of the references to color in this figure legend, the reader is referred to the Web version of this article.)

target HPPD in other organisms.

A three-dimensional model of *An. stephensi* HPPD shows these conserved features (Fig. 1B) as well as the typical HPPD fold: an 8-bladed β -propeller with the active site deeply buried and coordinated by the His183-His266-Glu349 triad. Docking known inhibitors into the model confirmed that mosquito HPPD can accommodate these molecules similarly to HPPD from plants and mammals. Overall, the conservation of the inhibitor-binding pocket suggests that existing HPPD-targeting chemistries (herbicides or drugs) could be repurposed to inhibit *An. stephensi* HPPD effectively.

2.2. Structural dynamics supports strong nitisinone binding to mosquito HPPD

We conducted *in-silico* inhibitor binding (Supplementary Fig. S2) and molecular dynamics (MD) simulations to further examine how inhibitors may interact with mosquito HPPD at the atomic level. We focused on two inhibitors with divergent efficacies: the triketone nitisinone (potent herbicide and human drug) and the less potent compound isoxaflutole (a pro-herbicide that converts to an active diketonitrile). The top inhibitor binding conformation (Supplementary Fig. S2) in the MD simulations revealed that nitisinone forms a stable bidentate interaction with the mosquito HPPD active site ion cofactor via its diketonate moiety, and remains bound within the pocket for the duration of the simulation (Fig. 2A and B). The conserved His183, His266, Glu349 triad coordinates the cofactor and indirectly anchors nitisinone in place, while Phe336 and Phe364 form the expected π -stacking interactions with the inhibitor's aromatic rings. In contrast, isoxaflutole exhibits higher transient interactions. During the MD simulation, isoxaflutole was

observed to drift and partially exit the binding pocket ("repelled" from the active site) (Fig. 2C). We reason that nitisinone's cyclohexane ring makes robust hydrophobic contacts (e.g., with Val185, Val228, Pro239, Phe359) and its nitro-trifluoromethylbenzoyl group conforms near Leu323 and Leu367, whereas isoxaflutole's smaller core and lack of a bulky aromatic tail results in weaker van der Waals interactions (Fig. 2D). The isoxaflutole escape mechanism causes high root mean square deviation (RMSD) of the alpha-helix 9 (residues Gly358 – Asn 376 in the human HPPD and residues Gly358 – Leu 381 in the *An. stephensi* HPPD) during the first 150 ns and the last 400 ns of MD (Supplemental Fig. S3A). Isoxaflutole causes the alpha-helix 9 to fold towards the open position while the nitisinone-bound HPPD remains similarly to the closed position (Supplemental Fig. S3B). These MD results provide a molecular support high affinity interaction of triketones, like nitisinone, with HPPD homologues of mosquitoes.

2.3. Nitisinone is a highly potent inhibitor of *An. stephensi* HPPD

To experimentally validate mosquito HPPD as a druggable target, we expressed *An. stephensi* and *An. gambiae* HPPD in *Escherichia coli* and tested a panel of six HPPD inhibitors representing major chemical classes (triketones, pyrazolones, isoxazoles) in the cell-based assay (Neuckermans et al., 2019) (Fig. 3A). The bacterial colorimetric assay provided a clear readout of HPPD inhibition: active soluble HPPD produced brown pigment (pyomelanin) secreted in the culture medium, whereas successful inhibition kept the medium pale (Fig. 3A and B). Dose-response curves were obtained for each compound for HPPD of *An. stephensi* and *An. gambiae* (Fig. 3C, Supplementary Fig. S4). Nitisinone and sulcotrione (both triketone inhibitors) outperformed all others by

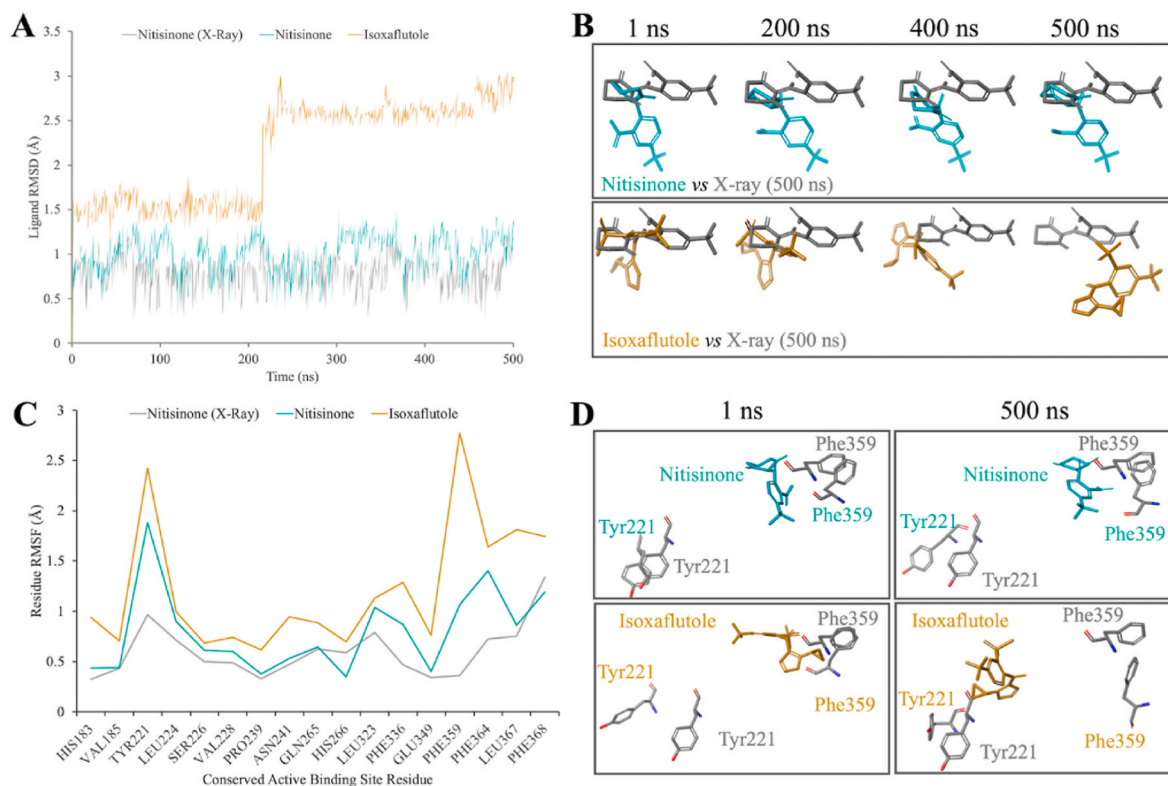


Fig. 2. MD simulations of *An. stephensi* HPPD predicted structure with inhibitors. (A) The root mean square deviation (RMSD; y-axis) of the resolved, x-ray data on nitisinone bound to the human HPPD (grey), or simulated data on *An. stephensi* HPPD potential inhibitor (cyan = nitisinone (predicted, positive control); tan = isoxaflutole), during the 500 ns MD (x-axis) with (B) respective images at specific time points of inhibitor conformations. (C) The active site escape mechanism of isoxaflutole caused a higher root mean square fluctuation (RMSF) in *An. stephensi* HPPD. The RMSF (y-axis) of the conserved active binding site residues (x-axis) during the 500 ns MD. (D) The images depict the *An. stephensi* HPPD residues (with respective colored labels) and the proximity of inhibitor conformations compared to the human HPPD conserved residues (grey labels). As a standard for the images, the final MD conformation (i.e., at 500 ns) was used to represent the human HPPD-nitisinone. (For interpretation of the references to color in this figure legend, the reader is referred to the Web version of this article.)

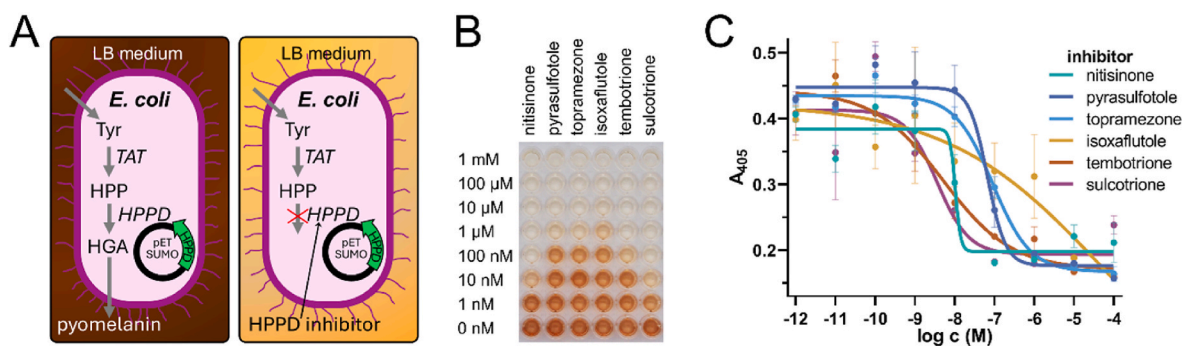


Fig. 3. Screening for mosquito HPPD inhibitors among selected commercially available HPPD inhibitors using a *E. coli* cellular assay. (A) Schematic representation of the bacterial assay used for screening HPPD inhibitors. *Escherichia coli* can convert tyrosine (Tyr) by its enzyme transaminases (TAT) into 4-hydroxyphenylpyruvate (HPP). HPP is then converted by mosquito HPPD, expressed from a pET SUMO expression vector with the inserted mosquito HPPD coding sequence, into homogentisic acid (HGA), which polymerizes to form characteristic brown pigment, pyomelanin, leading to dark coloration of LB medium (left part). In the presence of an HPPD inhibitor, this conversion is blocked, resulting in a lack of pigmentation and normal medium color (right part). (B) Photograph of a 96-well plate used in the screening assay of supernatant from *E. coli* culture expressing HPPD of *An. stephensi*. Each column represents a different inhibitor, and each row represents a different inhibitor concentration, ranging from 1 nM to 1 mM. Lighter wells indicate inhibition of HPPD. Last row represents the negative (solvent) control. (C) Dose-response curves of each tested compound, based on the 96-well plate shown in panel B. Absorbance of individual wells was measured at a wavelength of 405 nm. All wells were prepared in triplicates. The error bars represent the SEM. (For interpretation of the references to color in this figure legend, the reader is referred to the Web version of this article.)

roughly an order of magnitude, yielding IC_{50} values in the low nanomolar range (approximately 10 nM and 13 nM for nitisinone of *An. stephensi* and *An. gambiae*, respectively). In contrast, the other tested herbicides (tembotrione, topramezone, pyrasulfotole, isoxaflutole) exhibited IC_{50} values in the high nanomolar to micromolar range. The success of nitisinone and sulcotrione reinforces that the triketone chemotype is particularly well-suited to engaging the mosquito HPPD active site. This insight can guide future structure-activity relationship explorations to optimize HPPD inhibitors for insecticidal use. These data validate our *in silico* prediction that mosquito HPPD's active site can be effectively bound by known HPPD inhibitors, and they underscore triketones as the most potent inhibitor in our test set.

2.4. Nitisinone causes swift lethality in blood-fed mosquitoes

To evaluate the insecticidal activity of nitisinone on *An. stephensi*, we have subjected the mosquitoes to membrane feeding assay with nitisinone supplemented in the blood meal (Fig. 4A). The data revealed that the LC_{50} values at 24, 48, and 72 h (658 ± 96 nM, 557 ± 91 nM, and 693 ± 91 nM, respectively) were comparable, with overlapping confidence intervals indicating a relatively fast mode of action (Fig. 4B). In order to test the action of nitisinone in a protein-free diet, we used a feeding solution with buffer composition that leads to sorting of the meal to the

midgut (Samish et al., 1995). The results show that mosquitoes offered a lethal concentration of nitisinone (2.5 μM, as defined by the dose-response curve, Fig. 4B) in a protein-free diet showed no significant mortality even at five days post-treatment (Fig. 4C, Supplementary Fig. S5). Our data further show that nitisinone has no effect on feeding rates of mosquitoes served protein-rich or protein-free diets (Supplementary Fig. S6). This pronounced differences demonstrate that nitisinone's lethality is strictly blood-meal dependent, requiring hours post-feeding to liberate an internal build-up of digested tyrosine to toxic levels.

2.5. High protein content sensitises mosquitoes to nitisinone toxicity

To pinpoint the blood component(s) enabling nitisinone toxicity, we supplemented midgut-sorted diets with individual blood constituents plus 2.5 μM nitisinone, a dose lethal in whole-blood meals, and monitored mosquito post-feeding survival (Fig. 5A). Mosquitoes fed on whole blood supplemented with a lethal concentration of nitisinone (2.5 μM) exhibited swift mortality (71 % within 24 h, 91–94 % within 48–72 h after feeding), while those fed on serum showed similar survival rate to the control group within first 24 h and only 26–37 % mortality within 48–72 h after feeding. This suggests that an abundant protein present in red blood cells, such as haemoglobin, could be responsible for the

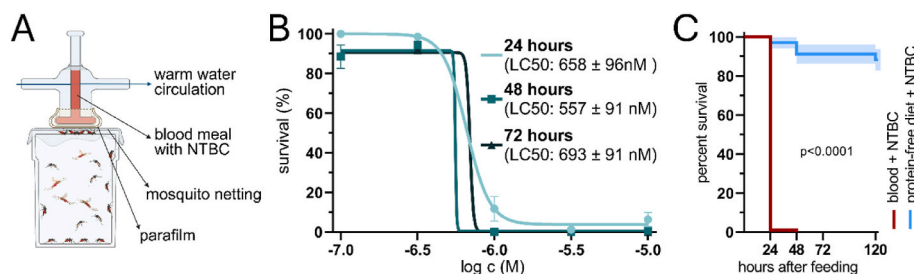


Fig. 4. (A) Membrane feeder assay used for mosquito feeding with bloodmeal and protein-free diet containing nitisinone (NTBC). (B) Dose-response curves show the nitisinone-induced post-feeding mortality of mosquitoes fed via membrane feeding on blood at 24, 48, and 72 h. Triplicates were conducted, with $n > 20$ per group. Means and SEMs are shown. The curve was generated in GraphPad Prism using the “log(inhibitor) vs. response - variable slope (four parameters)” model. (C) Comparison to protein-free diet feeding shows that nitisinone toxicity is dependent on protein presence in the diet. Mosquitoes fed on blood with a lethal concentration of nitisinone (2.5 μM) experienced almost 100 % mortality within 24 h and total mortality by 48 h, while those fed a protein-free diet showed survival rates close to 100 % up to 120 h. Survival curves were generated using Kaplan-Meier analysis with pooled data from three replicates containing a total of at least 34 fed mosquitoes, the P values were determined by the log-rank (Mantel-Cox), and error bars represent the standard error of survival probability estimates based on the binomial distribution. Detailed bar graphs from data shown in panel C are available in Supplementary Fig. S5.

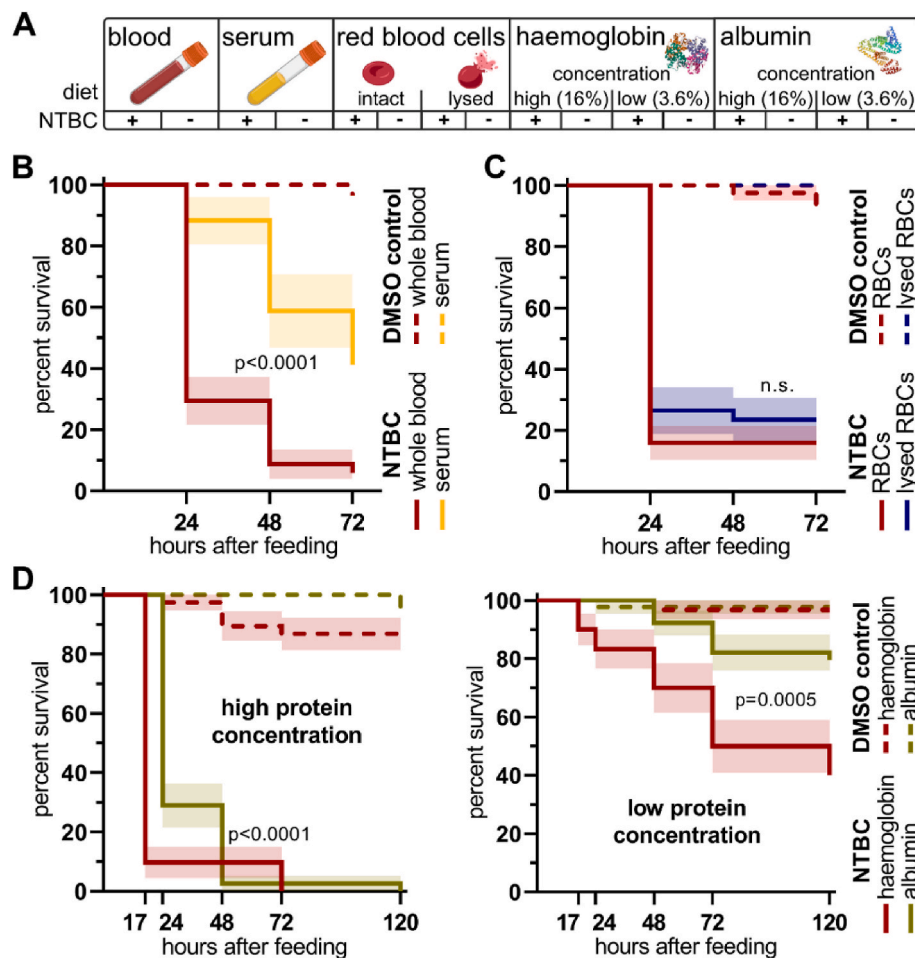


Fig. 5. Nitisinone-induced mosquito mortality under varying dietary conditions. Mosquitoes were fed via membrane feeding on varying diets. In all survival graphs, survival curves were generated using Kaplan-Meier analysis with pooled data from different replicates, the P-values were determined by the log-rank (Mantel-Cox), and error bars represent the standard error of survival probability estimates based on the binomial distribution. (A) **An overview of dietary components tested in mosquito survival experiments.** Each diet was tested with a lethal (2.5 μ M) concentration of nitisinone (nitisinone⁺) or 0.25 % DMSO as a solvent control (nitisinone⁻). (B) **Nitisinone quickly kills mosquitoes fed on whole blood, whereas serum-fed mosquitoes were killed by nitisinone with a delay.** Each group consisted of at least 27 fed mosquitoes. (C) **Survival comparison of mosquitoes fed on intact versus lysed red blood cells with nitisinone.** Each group consisted of at least 34 fed mosquitoes. Both panels B and C present pooled data from experiments using two different blood sources: human and bovine. For data from individual repetitions, see [Supplementary Fig. S7](#). (D) **Nitisinone causes faster mortality when served with haemoglobin than with albumin.** Mosquitoes were fed on a protein-free diet supplemented with haemoglobin or albumin at high or low concentrations, each supplemented with nitisinone (2.5 μ M). Each group consisted of 30–44 mosquitoes in total across three replicates. Detailed bar graphs from data shown in panels C and D including individual statistics are available in [Supplemental Fig. S5](#). (For interpretation of the references to color in this figure legend, the reader is referred to the Web version of this article.)

nitisinone-induced mortality (Fig. 5B). Mosquitoes fed on either intact or lysed red blood cells (RBCs) supplemented with nitisinone exhibited high mortality, comparable to that observed with whole blood, with no significant difference between the intact and lysed RBC treatments (Fig. 5C). We further tested, whether the protein type, and not only the protein quantity, determines the extent of HPPD inhibition phenotype. We thus fed mosquitoes nitisinone suspended in solution with haemoglobin and albumin, representing the main proteins in red blood cells and serum, respectively, each at two concentrations: high (16 %, w/vol) and low (3.6 %, w/vol), reflecting their approximate physiological levels of haemoglobin in blood (160 g/L) and albumin in serum (36 g/L). The results showed comparable killing rates between diets with high concentrations of either haemoglobin or albumin, with slightly faster killing on the haemoglobin diet (Fig. 5D, left part, [Supplementary Fig. S5](#)). At low protein concentrations, nitisinone resulted in 50 % mortality within 3 days in the presence of haemoglobin, whereas low concentration of albumin had survival rates similar to the control group without nitisinone (Fig. 5D, right part). These experiments indicate that the killing effect of nitisinone depends on a high protein content in the bloodmeal,

with a slightly higher toxicity in the presence of haemoglobin. Altogether, our results show that nitisinone's toxicity is mediated by blood proteins and thus acts specifically against blood-feeding insects.

2.6. Nitisinone's toxicity is not due to absence of downstream products of tyrosine catabolism

To assess whether the lethality of nitisinone results from a deficiency of downstream metabolites or from the toxic accumulation of upstream intermediates or tyrosine itself, we supplemented the bloodmeal with homogentisic acid (HGA), the direct product of HPPD. However, HGA addition at concentrations ranging from 6.25 to 50 mM failed to rescue normal survival and none of the HGA-supplemented groups approached the survival observed in non-treated controls (Fig. 6A, [Supplementary Table S1](#)). These results indicate that HGA supplementation does not counteract nitisinone-induced lethality, indicating that mortality is likely the result of accumulation of upstream metabolites rather than a lack of homogentisic acid.

To test whether oxidative stress resulting from tyrosine or

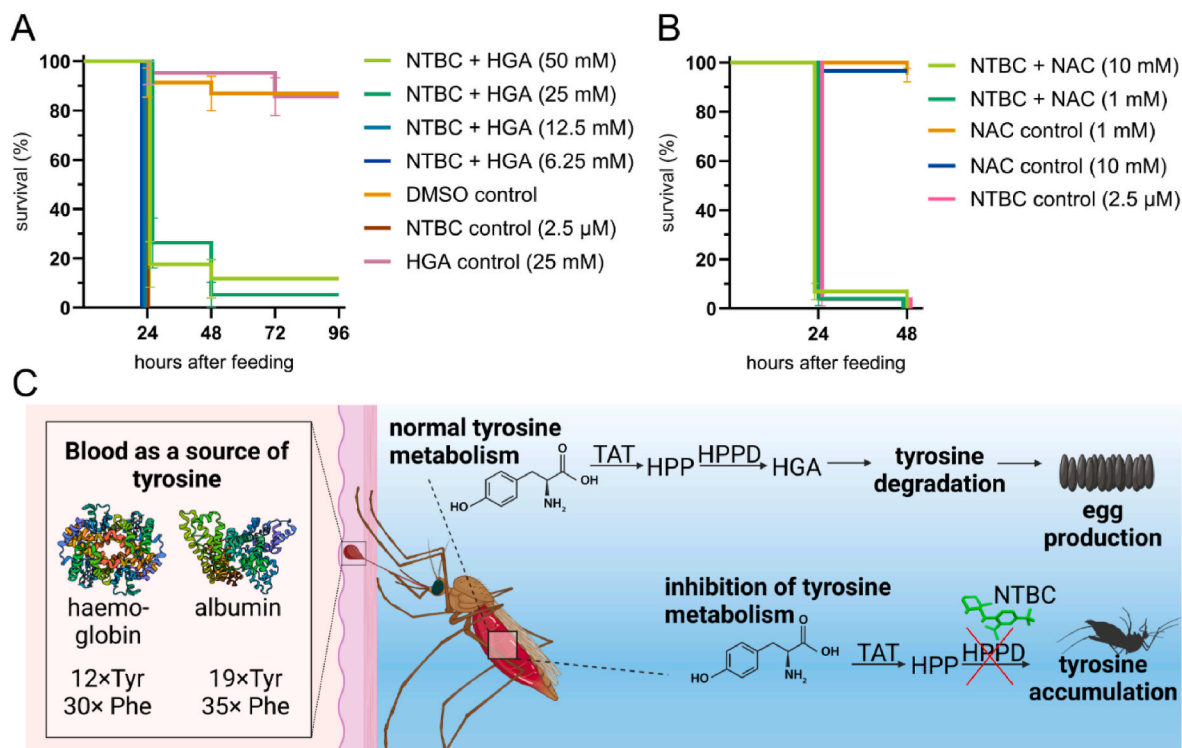


Fig. 6. (A) Exogenous homogentisic acid (HGA) does not rescue mosquito survival following nitisinone-spiked blood meal. Mosquitoes were fed via membrane feeding on blood supplemented with a lethal concentration of nitisinone (NTBC, 2.5 μ M), with and without homogentisic acid (HGA) at various concentrations (6.25–50 mM). Survival was monitored at 24 h, 48 h, 72 h, and 96 h post feeding. While HGA alone had no toxic effect, its co-administration with nitisinone failed to restore survival to control levels. Survival curves were generated using Kaplan-Meier analysis. Each group consisted of 17–25 fed mosquitoes. Error bars represent the standard error of survival probability estimates based on the binomial distribution. Log-rank testing showed no difference between non-NTBC control groups ($p = 0.9468$) and a significant difference ($p < 0.0001$) between all NTBC-containing groups and the HGA-only control. **(B) N-acetylcysteine (NAC) does not protect mosquitoes from nitisinone-induced lethality.** Mosquitoes were fed via membrane feeding on blood supplemented with a lethal concentration of nitisinone (2.5 μ M) and NAC (10 mM and 1 mM). Mosquito survival was monitored at 24 h and 48 h after feeding. Controls included NAC alone (10 mM and 1 mM) and nitisinone alone (2.5 μ M). None of the tested NAC concentrations restored normal survival. Survival curves were generated using Kaplan-Meier analysis. Each group consisted of more than 50 mosquitoes in total across two replicates. Error bars represent the standard error of survival probability estimates based on the binomial distribution. Log-rank testing showed no significant difference between any NTBC + NAC groups and the NTBC-only control, while all NTBC-treated groups differed significantly ($p < 0.0001$) from NAC-only controls. **(C) A schematic overview of the proposed mechanism of nitisinone toxicity in mosquito females.** Haemoglobin and albumin are the two dominant blood proteins, comprising around 90–95 % of total blood protein by mass. In albumin, tyrosine and phenylalanine account for 8.9 % of amino acid residues, while in haemoglobin, they represent 7.1 %.

intermediate accumulation contributes to nitisinone-induced lethality, we supplemented the bloodmeal with N-acetylcysteine (NAC), an antioxidant that replenishes glutathione levels. Even when tested at 10 mM and 1 mM, NAC co-administration with 2.5 μ M nitisinone did not improve mosquito survival, compared to nitisinone alone (Fig. 6B–Supplementary Table S1).

We next examined how blood-derived amino acids contribute to nitisinone toxicity by analysing the tyrosine and phenylalanine content of haemoglobin and albumin, the two major blood proteins used in mosquito feeding. Despite its slightly lower content of these amino acids, haemoglobin consistently led to greater nitisinone toxicity when fed to mosquitoes. Human haemoglobin (tetrameric structure, MW = 64 kDa) contains 12 tyrosines and 30 phenylalanines per molecule (7.1 % of amino acids), while human albumin (MW = 66.5 kDa) contains 19 tyrosines and 35 phenylalanines per molecule (8.9 %). Despite the higher total tyrosine and phenylalanine content in albumin, nitisinone toxicity is greater when mosquitoes are fed haemoglobin than albumin. Together, these findings highlight that nitisinone toxicity in *An. stephensi* is conditioned by the presence of blood proteins, with haemoglobin playing a particularly significant role in mediating this effect (Fig. 6C).

3. Discussion

The enzyme 4-hydroxyphenylpyruvate dioxygenase (HPPD), integral

to tyrosine catabolism across aerobic organisms, has emerged as a pivotal target in both agronomic and medical domains, owing to its central role in plant pigment biosynthesis (Chen et al., 2024; Shaner, 2003) and its implications in human metabolic disorders (Lindstedt, 1992). Recent studies brought up the idea that disrupting tyrosine catabolism can specifically kill blood-feeding arthropods (Sterkel et al., 2016). In particular, Sterkel et al. showed that inhibition of tyrosine degradation (via silencing of HPPD or the upstream enzyme TAT) is lethal to blood-fed insects, as excess tyrosine accumulates to toxic levels fluxed in from digesting of large protein-rich blood meals (Sterkel et al., 2016). Moreover, the repurposing of nitisinone, an FDA-approved HPPD inhibitor, has demonstrated environmentally friendly insecticidal effects in other disease vectors. For example, RNAi-based target validation as well as toxicological profiles of several triketone HPPD inhibitors demonstrated high vulnerability of *Aedes aegypti* mosquitoes and *Amblyomma americanum* ticks to downregulation HPPD levels or inhibited activity, leading to post blood-feeding mortality in both species (McComic et al., 2023). Feeding or topically applying nitisinone to tsetse flies (vectors of African trypanosomiasis) also caused high mortality, whereas the same treatment had no adverse effect on non-target insects like bumblebees (Besansky et al., 2021). This approach of exploiting blood-meal-induced toxicity was proposed as an eco-friendly alternative to conventional neurotoxic insecticides (Sterkel et al., 2016). Notably, nitisinone is a clinical drug with established human safety

(used to treat hereditary tyrosinemia type I), which could facilitate its adoption in public health settings. An immediate advantage of nitisinone is that it can be deployed in combination with existing malaria interventions in novel ways. For example, mosquitocidal approaches, administering drugs to humans or animals to make their blood lethal to mosquitoes, have gained attention as a complementary malaria control strategy (Haines et al., 2025). The classic human-administered mosquitocidal often proposed is ivermectin, but ivermectin has a very limited half-life *in vivo*. Nitisinone offers a promising alternative: it has a much longer half-life in human blood than ivermectin, meaning its mosquitocidal effect endures for days to weeks after a single dose (Haines et al., 2025). A recent study showed that a single human-equivalent dose of nitisinone can render blood meals lethal to *Anopheles* mosquitoes for up to 16 days (Haines et al., 2025), far outlasting the effect of ivermectin. This could streamline the pathway toward evaluating it in field trials as a vector control measure. Importantly, this strategy exploits an ecological vulnerability of malaria vectors: their reliance on human blood meals. Urban-adapted, anthropophilic species such as *An. stephensi*, now invading African cities and breeding in man-made containers (Emiru et al., 2023) could be especially impacted, since high human population density and limited alternative hosts in urban environments mean more mosquitoes would ingest the drug. Consequently, community-wide coverage is crucial to knock down disease-transmitting mosquito populations to the point that it disrupts the life cycle of *Plasmodium* parasites and thus breaks the chain of infection. This being said, it needs to be stressed that nitisinone provides no direct protective benefit to the individual, only to the community, which poses challenges for compliance and ethical deployment. Chemical and biological safety profiles also warrant scrutiny as nitisinone's mechanism inevitably raises blood tyrosine levels in humans, carrying a risk of reversible tyrosinemia and associated side effects like eye irritation (keratopathy) (Emiru et al., 2023), although lower vector-control doses are expected to minimise these effects. While existing studies on nitisinone robustly demonstrate proof-of-principle efficacy, we propose that substantial opportunities remain for targeted organic chemistry research. Specifically, development of novel HPPD inhibitors with increased selectivity for arthropod HPPD enzymes could significantly enhance the therapeutic index, thereby optimising safety and effectiveness of future vector control interventions.

Here, we report the validation of 4-hydroxyphenylpyruvate dioxygenase as a new emerging insecticidal target in mosquitoes, and demonstrate that inhibiting this enzyme with triketones such as nitisinone can specifically kill female *An. stephensi* after they ingest a blood meal. Our findings build upon earlier work of HPPD in other blood-sucking insects (Besansky et al., 2021; Haines et al., 2025; Sterkel et al., 2016) and complement them with novel mechanistic insights. To the best of our knowledge, our data provide the first evidence that HPPD is a relevant target in *An. stephensi* mosquitoes, a malaria vector originating from Asia and rapidly spreading in Africa. We demonstrate distinct inhibitor profiles of *An. stephensi* HPPD, highlighting the notable preference for inhibition by triketone-based inhibitors, such as nitisinone.

Our findings also indicate that haemoglobin enhances the lethality mediated by nitisinone inhibition of mosquito HPPD, despite containing fewer trypsin cleavage sites and lower abundance of the aromatic substrates tyrosine and phenylalanine compared to albumin. This counter-intuitive observation may reflect subtle differences in proteolytic kinetics, enzyme-inhibitor complex stability, and associated metabolic fluxes. One possibility is that mosquito's proteolytic digestion is a critical determinant in bringing about the nitisinone-mediated phenotype. Early studies identified a two-phase proteolytic response, with initial secretion of early trypsin activating transcription of later protease genes, critical for optimal digestion of haemoglobin (Isoe et al., 2009; Noriega et al., 1996). Proteomic analyses reveal that mosquito blood-fed midguts are enriched in several endoproteases that may efficiently process haemoglobin (O'Donoghue et al., 2025; Ramirez et al., 2025).

This would assume that the turn-around time of proteolytic system of blood-fed mosquitoes may generate more free tyrosine molecules from haemoglobin, compared to albumin, ultimately fuelling, at enhanced rate, to the toxic build-up of non-catabolised tyrosine molecules. Another possibility is that HPPD, as a non-heme iron(II)-dependent dioxygenase, is catalytically functional strictly upon a conserved Fe (II)-coordinating 2-His-1-Glu triad in its active site, facilitating substrate turnover (Huang et al., 2016). Inhibition of HPPD by nitisinone could then occur primarily through tight binding and stabilisation of a catalytically inactive enzyme-inhibitor complex, mediated by iron chelation (Lin et al., 2019a). Consequently, enhanced iron availability, as from hemoglobin-derived heme degradation (Zhou et al., 2007), might potentiate the formation and stabilisation of this inhibited enzyme-substrate-iron complex, effectively sequestering the enzyme in a conformation conducive to prolonged inhibitor occupancy. This tight, stable interaction (enzyme-inhibitor-iron-substrate complex) strongly prevents alternative metabolic shunts, keeping the substrate trapped, leading to a rapid and pronounced accumulation of toxic intermediates and unprocessed tyrosine.

Taken together, our findings support a model in which blood feeding leads to a terminal metabolic overload in the mosquito, ultimately transforming a blood meal into a metabolic internal trap for mosquitoes vector (Kopáček and Perner, 2016). Here, we have collected molecular details of inhibition of mosquito HPPD, a promising and emerging target for malaria vectors, emphasising the triketone chemotype inhibitors as the most potent. Inhibition of this enzyme with the nitisinone, the repurposed drug, kills specifically blood-fed female mosquitoes, effectively turning their essential blood meal into a toxic overdose. We discovered that haemoglobin digestion is the key trigger of this vulnerability, highlighting a unique aspect of mosquito biology that can be exploited for selective control. This work not only deepens our understanding of mosquito metabolic physiology but also suggests a complementary options for novel strategies of vector controls.

4. Material and methods

4.1. Predicted structure preparation and in-silico HPPD inhibitor binding

First, the three-dimensional structure of *An. stephensi* HPPD was modeled using homology modeling (SWISS-MODEL) (Waterhouse et al., 2018). The primary amino acid sequence of mosquito HPPD was provided as the target, and the structure of human HPPD complexed with nitisinone was uploaded as a template in PDB format (PDB entry 8IM2). The model was built using the ProMod3 pipeline (Schneidman-Duhovny et al., 2021), which aligns the target sequence to the template, transfers conserved coordinates, and reconstructs insertions and deletions using a fragment library. Side chains were optimized, and the geometry of the model was refined with a force field. Model quality was evaluated using QMEANDisCo (Studer et al., 2020), and the final model was prepared as a monomer. Ligands present in the template structure were excluded due to insufficient conservation of binding sites. Resulting PDB file was visualised and labeled using the UCSF ChimeraX molecular modeling package (Meng et al., 2023). The HPPD structure from *An. stephensi* was also predicted with AlphaFold (Jumper et al., 2021). To select which predicted *An. stephensi* HPPD structure for further analyses, all five AlphaFold predicted structures were submitted to the SwissDock server (Grosdidier et al., 2011) using default parameters with an adjustment on inhibitor coordination according to nitisinone of human HPPD, PDB: 8IM2. Nitisinone was initially used for the SwissDock server. The second AlphaFold structure (Predicted Aligned Error: 0.76) produced the best fit nitisinone and was therefore this AlphaFold structure was also used to bind isoxaflutole *in-silico*. The SwissParam score (SP-dG), an approximation of the binding free energy of a ligand to a target generated by SwissDock, was used to plot the RMSD inhibitor conformations. After a structural alignment with the human HPPD, the inhibitor approximating the position of the resolved, x-ray nitisinone (~4.5 Å RMSD) was

selected for preparation and optimisation using the Maestro software package. Firstly, the hydrogen atoms were substituted, and local minimizations were performed to remove steric clashes. Secondly, the Protein Preparation Wizard (Madhavi Sastry et al., 2013) was then used to optimize the hydrogen-bond networks. As a final preparation step, each system was built for MD, using the Desmond software (Bowers et al., 2006), by solvating the optimized structures in a 10 Å³ orthorhombic box with a TIP3P water model (Jorgensen et al., 1983; Mahoney and Jorgensen, 2000), neutralized, and salted with 0.15 M NaCl.

4.2. Classical molecular dynamics

The CHARMM36 force field (Huang and MacKerell, 2013) was used to parameterize the protein-inhibitor complexes and ions. The Swiss-Param server (Zoete et al., 2011) built the topology and force field parameters for nitisinone (x-ray), nitisinone (predicted), and isoxaflutole. All MD simulations were performed with a GPU-accelerated workstation employing the Desmond software (Bowers et al., 2006). The Desmond protocol involves several steps for initial equilibration and a final MD production step conducted under isotropic conditions using an NPT ensemble coupled with a Nose-Hoover thermostat (Evans and Holian, 1985) and a Martyna-Tobias-Klein barostat (Martyna et al., 1994). The temperature was set at 300 K with a RESPA (Tuckerman et al., 1992) integrator at an inner time step of 2-fs. As a positive control, all MD simulations were compared with simulations from the experimentally determined human HPPD-nitisinone structure (PDB: 8IM2). Images were captured and MD simulations were analysed using the Chimera and Maestro software package (Schrödinger, 2024-2).

4.3. Heterologous expression of mosquito HPPD

Anopheles gambiae and *An. stephensi* HPPD (accession numbers XP_318007.3 and XP_035912472.1) were synthesised with codon usage optimized for expression in *E. coli* (Eurofins Genomics) and supplied in the pGEX-4T-1 vector. The genes were amplified (using the same set of primers for both species: forward 5'-ATGACCACCTACACCGATAAGG-3' and reverse 5'-TTACAGGTTGCCACGCTTCTCT-3') and subcloned into the Champion™ pET SUMO Expression System (Thermo Fisher Scientific, USA), and transformed into One Shot® Mach 1™-T1R Competent Cells (Thermo Fisher Scientific, USA). The sequence-verified construct was then transformed into *E. coli* OverExpress™ C43(DE3) Chemically Competent Cells (catalogue number CMC0019, Sigma-Aldrich, USA) and used for HPPD inhibitors cellular screens. Bacterial Bioassay was slightly modified from (Neuckermans et al., 2019). Three mL of LB-kanamycin-glucose medium (1 % tryptone, 0.5 % yeast extract, 1 % NaCl, 1 % glucose, kanamycin 50 ng/mL) was inoculated with *E. coli* OverExpress™ C43(DE3) Chemically Competent Cells (catalog number CMC0019, Sigma-Aldrich, USA) containing the Champion™ pET SUMO Expression vector with the inserted mosquito HPPD sequence. The culture was grown overnight at 30 °C. On the second day, the overnight culture was centrifuged at 500×g for 10 min, and the supernatants were discarded. The pellets were resuspended in 3 mL of fresh LB-kanamycin medium without glucose, and the OD₆₀₀ was measured. Approximately 100 µL of the resuspended culture was added to 10 mL of fresh LB-kanamycin medium without glucose to achieve an OD₆₀₀ of approximately 0.1. The culture was grown to the OD₆₀₀ of 0.6 at 30 °C, while shaking at 250 rpm, and then centrifuged at 500×g for 10 min. The resulting pellet was resuspended in 10 mL of an expression medium (LB-kanamycin +10 mg/mL tyrosine, 1 mM IPTG). The inhibitors used were: nitisinone (Career Henan Chemical Co., CAS 104206-65-7; Pyrasulfotole (Merck, Supelco, 32973); Topramezone (Merck, Supelco, 34225); Isoxaflutole (Merck, Supelco, 46437); Tembotrione (Merck, Supelco, 32766); Sulcotrione (Merck, Supelco, 46318). These were solubilised in DMSO as 1 nM–100 mM stock solutions, which were further diluted 100 × (1 µL of the inhibitor was added into 99 µL of the cell suspension in expression medium was added) in the flat-bottom

96-well plate. The plate was covered with a lid, sealed using parafilm, and incubated overnight at 37 °C while shaking at 250 rpm. The next day, the plate was centrifuged at 500×g for 15 min, and the supernatants were transferred to new empty plates. The absorbance at 405 nm was measured using a plate reader Infinite® 200 PRO (Tecan, Switzerland). All data were acquired in independent triplicates. GraphPad Prism software was used to calculate means and standard errors of the means (SEMs), and generate dose-response curves using the “log(inhibitor) vs. response - variable slope (four parameters)” model.

4.4. Mosquitoes

Adult female mosquitoes from a colony of *An. stephensi*, Nijmegen Sind-Kasur strain (Feldmann and Ponnudurai, 2008), were maintained on a filter-sterilised 5 % sugar solution in a controlled environment (26 °C, 80 % humidity, and a 12 h light/12 h dark cycle) following standard rearing procedures (Timinao et al., 2021).

4.5. Membrane feeder assays

A day prior to membrane feeding assay, 20–30 mosquitoes (3–5 days old) were transferred into a paper cup covered with mosquito netting. Access to their normal sugar solution was denied 4–6 h prior to the feeding assay. The cups were placed under a row of glass membrane feeders with a blood meal pre-warmed to 37 °C. The mosquitoes were allowed to feed for 10–30 min in the dark. After 1 h, unfed individuals were removed from the cups. Engorged individuals were kept at a temperature 26 °C with 80 % humidity, and their survival was monitored at least once every 24 h.

4.6. Diets preparation

Blood was sourced from the Sanquin Blood Bank. Serum was obtained by 2500×g centrifugation. Non-protein buffer for testing nitisinone effects with a protein-free diet was prepared as follows: 139 mM NaCl, 10 mM NaHCO₃, pH 7.3, 10 mM ATP (added just before feeding), and 2 % blue food dye (to recognise fed individuals). For blood-feeding assays, nitisinone was initially dissolved in DMSO at 10 mM to create a stock solution. From this, working solutions were prepared by 1:200 dilution in serum, allowing final 1:400 dilution, once red blood cells were added to serum (50 % vol/vol). This approach resulted in a final dilution factor of 1:400 for both nitisinone and DMSO. Control diets contained an equivalent volume of DMSO (0.25 % v/v) without nitisinone. The resulting diet was mixed to create a feeding diet. For non-blood diets, nitisinone was directly diluted 400 × from the stock solution. Lysed red blood cells were prepared by freezing and thawing the red blood cells, followed by centrifugation at 13,000×g for 10 min. To compare mosquito survival following feeding with a lethal concentration of nitisinone (2.5 µM; shown to be lethal in Fig. 4B) in serum versus red blood cells, and normal versus lysed red blood cells, the serum was diluted 1:1 with non-protein buffer, and red blood cells were also diluted 1:1 with the same buffer. The supernatant was collected and diluted 1:1 with the non-protein buffer. As a control, diets without nitisinone were prepared, with the equivalent volume of DMSO (1 µL per 400 µL of diet). Haemoglobin (catalog number H2625, Sigma-Aldrich, USA) and albumin (catalogue number PM-T1725, Biosera, France) diets were prepared both at two concentrations, 16 % and 3.6 %, approximating the physiological range of these proteins in human blood. Haemoglobin and albumin were both dissolved in a non-protein buffer containing either a lethal concentration of nitisinone (2.5 µM) or solvent (0.25 % DMSO) as a negative control.

4.7. Dose-response curves

Mosquitoes were fed via membrane feeders on nitisinone-containing blood prepared as described above at the following final concentrations:

10 μ M, 3.16 μ M, 1 μ M, 316 nM, and 100 nM. The number of dead mosquitoes in each group was recorded at 24, 48, and 72 h post-feeding. Survival curves for each timepoint were generated in GraphPad Prism using the 'log(inhibitor) vs. response - variable slope (four parameters)' model. The experiment was performed in three independent replicates.

4.8. Survival experiments

Mosquitoes were fed via membrane feeding on varying diets prepared as described above. The survival rates were observed at least every 24 h over 3–6 days. In all survival graphs, survival curves were generated using Kaplan-Meier analysis with pooled data from different replicates, the P-values were determined by the log-rank (Mantel-Cox), and error bars represent the standard error of survival probability estimates based on the binomial distribution. Group sizes for survival analyses ranged from 17 to over 50 mosquitoes per condition, depending on feeding success and experimental setup (see figure legends for full details).

4.9. Homogentisic acid (HGA) and N-acetylcysteine (NAC) rescue experiments

Mosquitoes (n = 30 per group) were fed via membrane feeding. Fully engorged mosquitoes were included in survival analyses. The HGA experiment was performed without replication, while the NAC rescue experiment was conducted in duplicate. Survival curves were generated in GraphPad Prism using Kaplan-Meier analysis.

HGA was added into the blood meal with nitisinone at the following concentrations: 50 mM, 25 mM, 12.5 mM, and 6.25 mM. Controls included blood supplemented with DMSO alone, nitisinone alone, and 25 mM HGA alone. Survival was monitored at the following time points: 24 h, 48 h, 72 h, and 96 h.

For NAC, a separate set of blood meals was supplemented with NAC at concentrations of 10 mM and 1 mM, with nitisinone. Controls included NAC alone (both concentrations) and nitisinone alone. Survival was monitored at 24 h and 48 h post-feeding.

CRediT authorship contribution statement

Matěj Kučera: Writing – review & editing, Visualization, Software, Methodology, Investigation, Formal analysis, Data curation. **David Hartmann:** Writing – review & editing, Visualization, Methodology, Investigation, Formal analysis, Data curation. **James J. Valdés:** Software, Methodology, Investigation. **Adéla Palusová:** Investigation. **Avinash Sheshachalam:** Methodology, Investigation. **Marnix Vlot:** Methodology, Investigation. **Martijn W. Vos:** Methodology, Investigation. **Koen J. Decheri:** Writing – review & editing, Supervision, Resources, Funding acquisition, Formal analysis. **Jan Perner:** Writing – review & editing, Writing – original draft, Supervision, Project administration, Funding acquisition, Formal analysis, Conceptualization.

Acknowledgment

This work was supported by the Czech Science Foundation (No: 22-18424M) and the Technology Agency of the Czech Republic (TREND Programme FW10010308).

Appendix A. Supplementary data

Supplementary data to this article can be found online at <https://doi.org/10.1016/j.ibmb.2025.104361>.

References

Basansky, N.J., Sterkel, M., Haines, L.R., Casas-Sánchez, A., Owino, Adung'a V., Vionette-Amaral, R.J., Quek, S., Rose, C., Silva dos Santos, M., García Escude, N.,

- et al., 2021. Repurposing the orphan drug nitisinone to control the transmission of African trypanosomiasis. *PLoS Biol.* 19.
- Bowers, K.J., Chow, D.E., Xu, H., Dror, R.O., Eastwood, M.P., Gregersen, B.A., Klepeis, J. L., Kolosvary, I., Moraes, M.A., Sacerdoti, F.D., et al., 2006. Scalable algorithms for molecular dynamics simulations on commodity clusters. *ACM/IEEE SC 2006 Conference (SC'06)*, pp. 43–43.
- Cerqueira de Araujo, A., Noel, B., Breteau, A., Labadie, K., Boudet, M., Tadrant, N., Istace, B., Kritli, S., Craud, C., Olaso, R., et al., 2025. Genome sequences of four ixodes species expands understanding of tick evolution. *BMC Biol.* 23.
- Chen, P., Niu, M., Qiu, Y., Zhang, Y., Xu, J., Wang, R., Wang, Y., 2024. Physiological effects of maize stressed by HPPD inhibitor herbicides via multi-spectral technology and two-dimensional correlation spectrum technology. *Ecotoxicol. Environ. Saf.* 272.
- Churcher, T.S., Lissenden, N., Griffin, J.T., Worrall, E., Ranson, H., 2016. The impact of pyrethroid resistance on the efficacy and effectiveness of bednets for malaria control in Africa. *eLife* 5.
- Emiru, T., Getachew, D., Murphy, M., Sedda, L., Ejigu, L.A., Bulto, M.G., Byrne, I., Demisse, M., Abdo, M., Chali, W., et al., 2023. Evidence for a role of *Anopheles stephensi* in the spread of drug- and diagnosis-resistant malaria in Africa. *Nat. Med.* 29, 3203–3211.
- Evans, D.J., Holian, B.L., 1985. The nose-hoover thermostat. *J. Chem. Phys.* 83, 4069–4074.
- Feldmann, A.M., Ponnudurai, T., 2008. Selection of *Anopheles stephensi* for refractoriness and susceptibility to *Plasmodium falciparum*. *Med. Vet. Entomol.* 3, 41–52.
- French-Constant, R.H., Williamson, M.S., Davies, T.G.E., Bass, C., 2016. Ion channels as insecticide targets. *J. Neurogenet.* 30, 163–177.
- Grosdidier, A., Zoete, V., Michielin, O., 2011. SwissDock, a protein-small molecule docking web service based on EADock DSS. *Nucleic Acids Res.* 39, W270–W277.
- Haines, L.R., Trett, A., Rose, C., García, N., Sterkel, M., McGuinness, D., Regnault, C., Barrett, M.P., Leroy, D., Burrows, J.N., et al., 2025. *Anopheles* mosquito survival and pharmacokinetic modeling show the mosquitocidal activity of nitisinone. *Sci. Transl. Med.* 17.
- Hancock, P.A., Ochomo, E., Messenger, L.A., 2024. Genetic surveillance of insecticide resistance in African *Anopheles* populations to inform malaria vector control. *Trends Parasitol.* 40, 604–618.
- Huang, J., MacKerell, A.D., 2013. CHARMM36 all-atom additive protein force field: validation based on comparison to NMR data. *J. Comput. Chem.* 34, 2135–2145.
- Huang, C.W., Liu, H.C., Shen, C.P., Chen, Y.T., Lee, S.J., Lloyd, M.D., Lee, H.J., 2016. The different catalytic roles of the metal-binding ligands in human 4-hydroxyphenylpyruvate dioxygenase. *Biochem. J.* 473, 1179–1189.
- Isoe, J., Rascón, A.A., Kunz, S., Miesfeld, R.L., 2009. Molecular genetic analysis of midgut serine proteases in *Aedes aegypti* mosquitoes. *Insect Biochem. Mol. Biol.* 39, 903–912.
- Jorgensen, W.L., Chandrasekhar, J., Madura, J.D., Impey, R.W., Klein, M.L., 1983. Comparison of simple potential functions for simulating liquid water. *J. Chem. Phys.* 79, 926–935.
- Jumper, J., Evans, R., Pritzel, A., Green, T., Figurnov, M., Ronneberger, O., Tunyasuvunakool, K., Bates, R., Židek, A., Potapenko, A., et al., 2021. Highly accurate protein structure prediction with AlphaFold. *Nature* 596, 583–589.
- Kopáček, P., Perner, J., 2016. Vector Biology: tyrosine Degradation Protects Blood Feeders from Death via La Grande Bouffe. *Curr. Biol.* 26, R763–R765.
- Lin, H.Y., Chen, X., Chen, J.N., Wang, D.W., Wu, F.X., Lin, S.Y., Zhan, C.G., Wu, J.W., Yang, W.C., Yang, G.F., 2019a. Crystal structure of 4-Hydroxyphenylpyruvate dioxygenase in complex with substrate reveals a new starting point for herbicide discovery. *Research* 2019, 2602414.
- Lin, H.Y., Yang, J.F., Wang, D.W., Hao, G.F., Dong, J.Q., Wang, Y.X., Yang, W.C., Wu, J. W., Zhan, C.G., Yang, G.F., 2019b. Molecular insights into the mechanism of 4-hydroxyphenylpyruvate dioxygenase inhibition: enzyme kinetics, x-ray crystallography and computational simulations. *FEBS J.* 286, 975–990.
- Lindstedt, S., 1992. Treatment of hereditary tyrosinaemia type I by inhibition of 4-hydroxyphenylpyruvate dioxygenase. *Lancet* 340, 813–817.
- Liu, Y.-X., Zhao, L.-X., Ye, T., Gao, S., Li, J.-Z., Ye, F., Fu, Y., 2020. Identification of key residues determining the binding specificity of human 4-hydroxyphenylpyruvate dioxygenase. *Eur. J. Pharmaceut. Sci.* 154.
- Madhavi Sastry, G., Adzhigirey, M., Day, T., Annabhimoju, R., Sherman, W., 2013. Protein and ligand preparation: parameters, protocols, and influence on virtual screening enrichments. *J. Comput. Aided Mol. Des.* 27, 221–234.
- Mahoney, M.W., Jorgensen, W.L., 2000. A five-site model for liquid water and the reproduction of the density anomaly by rigid, nonpolarizable potential functions. *J. Chem. Phys.* 112, 8910–8922.
- Martyna, G.J., Tobias, D.J., Klein, M.L., 1994. Constant pressure molecular dynamics algorithms. *J. Chem. Phys.* 101, 4177–4189.
- McComic, S.E., Duke, S.O., Burgess, E.R., Swale, D.R., 2023. Defining the toxicological profile of 4-hydroxyphenylpyruvate dioxygenase-directed herbicides to *Aedes aegypti* and *Amblyomma americanum*. *Pestic. Biochem. Physiol.* 194.
- Meng, E.C., Goddard, T.D., Pettersen, E.F., Couch, G.S., Pearson, Z.J., Morris, J.H., Ferrin, T.E., 2023. UCSF ChimeraX: tools for structure building and analysis. *Protein Sci.* 32.
- Neafsey, D.E., Waterhouse, R.M., Abai, M.R., Aganezov, S.S., Alekseyev, M.A., Allen, J. E., Amon, J., Arcà, B., Arensburger, P., Artemov, G., et al., 2015. Highly evolvable malaria vectors: the genomes of 16 *Anopheles* mosquitoes. *Science* 347.
- Neidig, M.L., Decker, A., Kavana, M., Moran, G.R., Solomon, E.I., 2005. Spectroscopic and computational studies of NTBC bound to the non-heme iron enzyme (4-hydroxyphenyl)pyruvate dioxygenase: active site contributions to drug inhibition. *Biochem. Biophys. Res. Commun.* 338, 206–214.

- Neuckermans, J., Mertens, A., De Win, D., Schwaneberg, U., De Kock, J., 2019. A robust bacterial assay for high-throughput screening of human 4-hydroxyphenylpyruvate dioxygenase inhibitors. *Sci. Rep.* 9.
- Noriega, F.G., Wang, X.-Y., Pennington, J.E., Barillas-Mury, C.V., Wells, M.A., 1996. Early trypsin, a female-specific midgut protease in *Aedes aegypti*: isolation, amino-terminal sequence determination, and cloning and sequencing of the gene. *Insect Biochem. Mol. Biol.* 26, 119–126.
- O'Donoghue, A.J., Liu, C., Simington, C.J., Montermoso, S., Moreno-Galvez, E., Serafim, M.S.M., Burata, O.E., Lucero, R.M., Nguyen, J.T., Fong, D., et al., 2025. Comprehensive proteolytic profiling of *Aedes aegypti* mosquito midgut extracts: unraveling the blood meal protein digestion system. *PLoS Neglected Trop. Dis.* 19.
- Ramirez, A.G., Isoe, J., Serafim, M.S.M., Fong, D., Le, M.A., Nguyen, J.T., Burata, O.E., Lucero, R.M., Spangler, R.K., Rascón, A.A., 2025. Biochemical and physiological characterization of *Aedes aegypti* midgut chymotrypsin. *Sci. Rep.* 15.
- Ribeiro, J.M.C., Genta, F.A., Sorgine, M.H.F., Logullo, R., Mesquita, R.D., Paiva-Silva, G. O., Majerowicz, D., Medeiros, M., Koerich, L., Terra, W.R., et al., 2014. An insight into the transcriptome of the digestive tract of the bloodsucking bug, *rhodnius prolixus*. *PLoS Neglected Trop. Dis.* 8.
- Samish, M., Kozłowska, A., Maramorosch, K., 1995. Factors affecting membrane feeding of *Anopheles stephensi*. *J. Am. Mosq. Control Assoc.* 11, 408–415.
- Schneidman-Duhovny, D., Studer, G., Tauriello, G., Bienert, S., Biasini, M., Johnner, N., Schwede, T., 2021. ProMod3—A versatile homology modelling toolbox. *PLoS Comput. Biol.* 17.
- Shaner, D.L., 2003. Herbicide safety relative to common targets in plants and mammals. *Pest Manag. Sci.* 60, 17–24.
- Sterkel, M., Perdomo Hugo, D., Guizzo Melina, G., Barletta Ana Beatriz, F., Nunes Rodrigo, D., Dias Felipe, A., Sorgine Marcos, H.F., Oliveira Pedro, L., 2016. Tyrosine detoxification is an essential trait in the life history of blood-feeding arthropods. *Curr. Biol.* 26, 2188–2193.
- Sterkel, M., Oliveira, J.H.M., Bottino-Rojas, V., Paiva-Silva, G.O., Oliveira, P.L., 2017. The dose makes the poison: nutritional overload determines the life traits of blood-feeding arthropods. *Trends Parasitol.* 33, 633–644.
- Studer, G., Rempfer, C., Waterhouse, A.M., Gumienny, R., Haas, J., Schwede, T., Elofsson, A., 2020. QMEANDisCo—distance constraints applied on model quality estimation. *Bioinformatics* 36, 1765–1771.
- Taylor, R., Messenger, L.A., Abeku, T.A., Clarke, S.E., Yadav, R.S., Lines, J., 2024. Invasive *Anopheles stephensi* in Africa: insights from Asia. *Trends Parasitol.* 40, 731–743.
- Timinao, L., Vinit, R., Katusale, M., Schofield, L., Burkot, T.R., Karl, S., 2021. Optimization of the feeding rate of *Anopheles farauti* s.s. colony mosquitoes in direct membrane feeding assays. *Parasites Vectors* 14.
- Toure, Y., Oduola, A.M.J., Carlos, M.M., 2004. The *Anopheles gambiae* genome: next steps for malaria vector control. *Trends Parasitol.* 20, 142–149.
- Tuckerman, M., Berne, B.J., Martyna, G.J., 1992. Reversible multiple time scale molecular dynamics. *J. Chem. Phys.* 97, 1990–2001.
- Venkatesan, P., 2024. The 2023 WHO world malaria report. *Lancet Microbe* 5.
- Waterhouse, A., Bertoni, M., Bienert, S., Studer, G., Tauriello, G., Gumienny, R., Heer, F. T., de Beer, T.A.P., Rempfer, C., Bordoli, L., et al., 2018. SWISS-MODEL: homology modelling of protein structures and complexes. *Nucleic Acids Res.* 46, W296–W303.
- Zhou, G., Kohlhepp, P., Geiser, D., Frasquillo Mdél, C., Vazquez-Moreno, L., Winzerling, J.J., 2007. Fate of blood meal iron in mosquitoes. *J. Insect Physiol.* 53, 1169–1178.
- Zoete, V., Cuendet, M.A., Grosdidier, A., Michielin, O., 2011. SwissParam: a fast force field generation tool for small organic molecules. *J. Comput. Chem.* 32, 2359–2368.